



# Ultraslow optical solitons and their storage and retrieval in an ultracold ladder-type atomic system

Yang Chen, Zhengyang Bai, and Guoxiang Huang\*

*State Key Laboratory of Precision Spectroscopy and Department of Physics, East China Normal University, Shanghai 200062, China*

(Received 14 January 2014; published 21 February 2014)

We propose a scheme to obtain stable nonlinear optical pulses and realize their storage and retrieval in an ultracold ladder-type three-level atomic gas via electromagnetically induced transparency. Based on Maxwell-Bloch equations we derive a nonlinear equation governing the evolution of the probe-field envelope and show that optical solitons with an ultraslow propagating velocity and extremely low generation power can be created in the system. Furthermore, we demonstrate that such ultraslow optical solitons can be stored and retrieved by switching a control field off and on. Due to the balance between dispersion and nonlinearity, the ultraslow optical solitons are robust during propagation, and hence their storage and retrieval are more desirable than those of linear optical pulses. This raises the possibility of realizing the storage and retrieval of light and quantum information by using solitonic pulses.

DOI: [10.1103/PhysRevA.89.023835](https://doi.org/10.1103/PhysRevA.89.023835)

PACS number(s): 42.65.Tg

## I. INTRODUCTION

In recent years, much effort has been paid to the study of electromagnetically induced transparency (EIT), a typical quantum interference effect occurring in resonant multi-level atomic systems. The light propagation in EIT systems possesses many striking features, including a substantial suppression of optical absorption, significant reduction of group velocity, and giant enhancement of Kerr nonlinearity. Based on these features, many applications of nonlinear optical processes at a weak light level can be realized [1].

One of the important applications of EIT is light storage and retrieval, which can be explained by the concept of the dark-state polariton [2], a combination of atomic coherence and probe pulse. The dark-state polariton prominently shows an atomic character when a control field is switched off and an optical character when the control field is switched on. The storage and retrieval of probe pulses based on EIT have been verified in many experiments [3–15].

However, up to now most previous works on light storage and retrieval based on EIT have been carried out in  $\Lambda$ -type three-level atomic systems. In addition, the probe pulse used is very weak and hence the system works in a linear regime, except for the numerical study presented in Ref. [16]. It is known that linear probe pulses suffer a spreading and attenuation due to the existence of dispersion, which may result in a serious distortion for retrieved pulses. For practical applications, it is desirable to obtain optical pulses that are robust during storage and retrieval.

In this article, we propose a scheme to produce stable weak nonlinear optical pulses and realize their robust storage and retrieval. The system we consider is an ultracold atomic gas with a ladder-type three-level configuration working under EIT conditions. Starting from Maxwell-Bloch (MB) equations we derive a nonlinear Schrödinger (NLS) equation governing the evolution of the probe-field envelope and show that optical solitons with an ultraslow propagating velocity and extremely low generation power can be created in the system. Furthermore, we demonstrate that such ultraslow optical

solitons can be stored and retrieved by switching a control field off and on. Due to the balance between dispersion and nonlinearity, the ultraslow optical solitons are robust during propagation, and hence their storage and retrieval are more desirable than those of linear optical pulses.

Before preceding, we note that, on the one hand, recently much attention has focused on ultracold Rydberg atoms [17,18] due to their intriguing properties, useful for quantum information processing and nonlinear optical processes; on the other hand, ultraslow optical solitons via EIT have been predicted for  $\Lambda$ -type three-level atoms [19,20]. In a recent work Maxwell *et al.* reported the storage of weak (i.e., linear) probe pulses in a ladder-type system using ultracold Rydberg atoms [21]. However, to the best of our knowledge, till now there has been no report on the storage and retrieval of ultraslow optical solitons in ladder-type atomic systems. Our theoretical results given here raise the possibility of realizing the storage and retrieval of light and quantum information by using nonlinear solitonic pulses. Experimentally, it is hopeful to employ low-density ultracold Rydberg atoms, where the Rydberg state has a very long lifetime [17,18], to realize the storage and retrieval of the ultraslow optical solitons predicted in our work.

The article is arranged as follows. In Sec. II, the physical model under study is described. In Sec. III, a derivation of the NLS equation controlling the evolution of the probe-field envelope is given, and ultraslow optical soliton solutions and their interaction are presented. In Sec. IV, the storage and retrieval of the ultraslow optical solitons are investigated in detail. Finally, the last section presents a summary of the main results of our work.

## II. MODEL

We consider a life-broadened three-level atomic system with a ladder-type level configuration [Fig. 1(a)], where  $|1\rangle$ ,  $|2\rangle$ , and  $|3\rangle$  are ground, intermediate, and upper states, respectively. Especially, state  $|3\rangle$  can be taken as a Rydberg state that has a very long lifetime. We assume that the atoms work in an ultracold (e.g.,  $\mu\text{K}$ ) environment so that their center-of-mass motion can be ignored. A probe field of center angular frequency  $\omega_p$  couples to the transition  $|1\rangle \rightarrow |2\rangle$  and

\*gxhuang@phy.ecnu.edu.cn

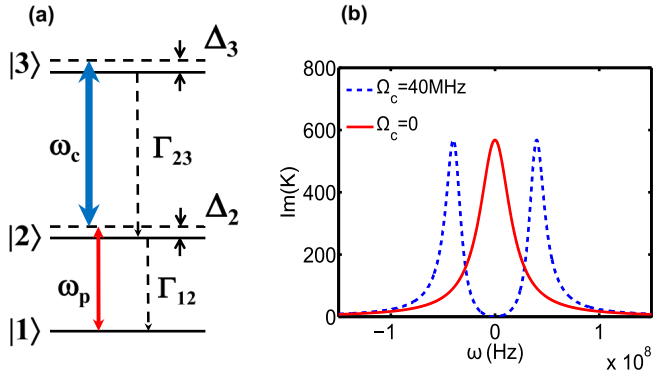


FIG. 1. (Color online) (a) Energy-level diagram and excitation scheme of the three-level ladder-type atoms, in which states  $|2\rangle$  and  $|1\rangle$  are coupled by the probe field with angular frequency  $\omega_p$ , and states  $|3\rangle$  and  $|2\rangle$  are coupled by the control field with angular frequency  $\omega_c$ .  $\Delta_2$  and  $\Delta_3$  are, respectively, one- and two-photon detunings;  $\Gamma_{13}$  ( $\Gamma_{23}$ ) is the spontaneous emission decay rate from  $|3\rangle$  to  $|1\rangle$  (from  $|3\rangle$  to  $|2\rangle$ ). (b) Absorption spectrum  $\text{Im}(K)$  of the probe field as a function of  $\omega$ . Solid and dashed lines correspond, respectively, to  $\Omega_c = 0$  (no EIT) and  $\Omega_c = 40$  MHz (EIT).

a control field of center angular frequency  $\omega_c$  couples to the transition  $|2\rangle \rightarrow |3\rangle$ .

For simplicity, we assume that both the probe and the control fields propagate along the  $z$  direction. Then the electric field of the system can be expressed as  $\mathbf{E} = \sum_{l=p,c} \mathbf{e}_l \mathcal{E}_l \exp[i(k_l z - \omega_l t)] + \text{c.c.}$  Here  $\mathbf{e}_p$  and  $\mathbf{e}_c$  ( $\mathcal{E}_p$  and  $\mathcal{E}_c$ ) are, respectively, the polarization unit vectors (envelopes) of the probe and control fields;  $k_p = \omega_p/c$  and  $k_c = \omega_c/c$  are, respectively, the wave numbers of the probe and control fields before entering the medium.

Under electric-dipole and rotating-wave approximations, the equations of motion for the density matrix elements in the interaction picture read [22]

$$\frac{\partial}{\partial t} \sigma_{11} = i\Omega_p^* \sigma_{21} - i\Omega_p \sigma_{21}^* + \Gamma_{12} \sigma_{22}, \quad (1a)$$

$$\begin{aligned} \frac{\partial}{\partial t} \sigma_{22} = & i\Omega_p \sigma_{21}^* + i\Omega_c^* \sigma_{32} - i\Omega_p^* \sigma_{21} - i\Omega_c \sigma_{32}^* \\ & - \Gamma_{12} \sigma_{22} + \Gamma_{23} \sigma_{33}, \end{aligned} \quad (1b)$$

$$\frac{\partial}{\partial t} \sigma_{33} = i\Omega_c \sigma_{32}^* - i\Omega_c^* \sigma_{32} - \Gamma_{33} \sigma_{33}, \quad (1c)$$

$$\frac{\partial}{\partial t} \sigma_{21} = id_{21} \sigma_{21} + i\Omega_p (\sigma_{11} - \sigma_{22}) + i\Omega_c^* \sigma_{31}, \quad (1d)$$

$$\frac{\partial}{\partial t} \sigma_{31} = id_{31} \sigma_{31} - i\Omega_p \sigma_{32} + i\Omega_c \sigma_{21}, \quad (1e)$$

$$\frac{\partial}{\partial t} \sigma_{32} = id_{32} \sigma_{32} + i\Omega_c (\sigma_{22} - \sigma_{33}) - i\Omega_p^* \sigma_{31}, \quad (1f)$$

where  $\Omega_p = (\mathbf{e}_p \cdot \mathbf{p}_{21}) \mathcal{E}_p / \hbar$  and  $\Omega_c = (\mathbf{e}_c \cdot \mathbf{p}_{32}) \mathcal{E}_c / \hbar$  are, respectively, the half-Rabi frequencies of the probe and the control fields, with  $\mathbf{p}_{ij}$  the electric dipole matrix element associated with the transition between  $|j\rangle$  and  $|i\rangle$ . In Eq. (1),  $d_{21} = \Delta_2 + i\gamma_{21}$ ,  $d_{31} = \Delta_3 + i\gamma_{31}$ , and  $d_{32} = (\Delta_3 - \Delta_2) + i\gamma_{32}$ , with  $\Delta_2 = \omega_p - (\omega_2 - \omega_1)$  and  $\Delta_3 = \omega_p + \omega_c - (\omega_3 - \omega_1)$ , respectively, the one-photon and two-photon detunings;

$\gamma_{ij} = (\Gamma_i + \Gamma_j)/2 + \gamma_{ij}^{\text{col}}$ ,  $\Gamma_j = \sum_{i < j} \Gamma_{ij}$ , with  $\Gamma_{ij}$  denoting the spontaneous emission decay rate from  $|j\rangle$  to  $|i\rangle$  and  $\gamma_{ij}^{\text{col}}$  denoting the dephasing rate between state  $|i\rangle$  and state  $|j\rangle$  [23].

The evolution of the electric field is governed by the Maxwell equation, which, under a slowly varying envelope approximation, yields [24]

$$i \left( \frac{\partial}{\partial z} + \frac{1}{c} \frac{\partial}{\partial t} \right) \Omega_p + \kappa_{12} \sigma_{21} = 0, \quad (2a)$$

$$i \left( \frac{\partial}{\partial z} + \frac{1}{c} \frac{\partial}{\partial t} \right) \Omega_c + \kappa_{23} \sigma_{32} = 0, \quad (2b)$$

where  $\kappa_{12} = \mathcal{N}_a \omega_p |\mathbf{p}_{12}|^2 / (2\epsilon_0 c \hbar)$  and  $\kappa_{23} = \mathcal{N}_a \omega_c |\mathbf{p}_{23}|^2 / (2\epsilon_0 c \hbar)$ , with  $\mathcal{N}_a$  the atomic density. Note that for simplicity we have assumed that both the probe and the control fields have a large beam radius in both the  $x$  and the  $y$  directions so that the diffraction effect represented by the term  $(\partial^2 / \partial x^2 + \partial^2 / \partial y^2) \Omega_{p,c}$  can be neglected.

### III. ULTRASLOW OPTICAL SOLITONS

#### A. Nonlinear envelope equation

We first consider the formation and propagation of ultraslow optical solitons in the system. We assume that the probe field is weakly nonlinear and pulsed with time duration  $\tau_0$ ; the control field is a continuous wave (i.e., its time duration is much larger than  $\tau_0$ ) and is strong enough so that its depletion can be neglected during propagation, which means that  $\Omega_c$  can be taken as a constant and hence Eq. (2b) can be disregarded.

In order to derive the nonlinear envelope equation of the probe field, we make the asymptotic expansion  $\sigma_{jl} = \sigma_{jl}^{(0)} + \epsilon \sigma_{jl}^{(1)} + \epsilon^2 \sigma_{jl}^{(2)} + \epsilon^3 \sigma_{jl}^{(3)} + \dots$ ,  $\Omega_p = \epsilon \Omega_p^{(1)} + \epsilon^2 \Omega_p^{(2)} + \epsilon^3 \Omega_p^{(3)} + \dots$ , with  $\sigma_{jl}^{(0)} = \delta_{jl} \delta_{l1}$  and  $\epsilon$  a small parameter characterizing the amplitude of  $\Omega_p$ . To obtain a divergence-free expansion, all quantities on the right-hand side of the expansion are considered as functions of the multiscale variables  $z_l = \epsilon^l z$  ( $l = 0, 1, 2$ ) and  $t_l = \epsilon^l t$  ( $l = 0, 1$ ).

Substituting the above expansion to the MB Eqs. (1) and (2a) and comparing the coefficients of  $\epsilon^l$  ( $l = 1, 2, 3, \dots$ ), we obtain a set of linear but inhomogeneous equations which can be solved order by order. At first order, we obtain the solution

$$\Omega_p^{(1)} = F e^{i\theta}, \quad (3a)$$

$$\sigma_{21}^{(1)} = \frac{\omega + d_{31}}{D(\omega)} F e^{i\theta}, \quad (3b)$$

$$\sigma_{31}^{(1)} = -\frac{\Omega_c}{D(\omega)} F e^{i\theta}, \quad (3c)$$

with other  $\sigma_{jl}^{(1)} = 0$ . In the above expressions,  $D(\omega) = |\Omega_c|^2 - (\omega + d_{21})(\omega + d_{31})$ ,  $\theta = K(\omega)z_0 - \omega t_0$  [25], with  $F$  the envelope function of the slow variables  $z_1, z_2$ , and  $t_1$ ;  $K(\omega)$  is the linear dispersion relation of the system, given by

$$K(\omega) = \frac{\omega}{c} + \frac{\kappa_{12}(\omega + d_{31})}{D(\omega)}. \quad (4)$$

Figure 1(b) shows  $\text{Im}(K)$ , i.e., the imaginary part of  $K$ , as a function of  $\omega$ . When plotting the figure, we chose ultracold

Rydberg atoms with the levels in Fig. 1(a) and the system parameters as [21,26] follows:

$$\begin{aligned} |1\rangle &= |5s^2S_{1/2}, F=2\rangle, & |2\rangle &= |5p^2P_{3/2}, F=3\rangle, \\ |3\rangle &= |60s^2S_{1/2}, \rangle. \end{aligned} \quad (5)$$

$$\begin{aligned} \Gamma_{12}/2\pi &= 6 \text{ MHz}, & \Gamma_{23}/2\pi &= 3200 \text{ Hz}, \\ \gamma_{21} &\approx 18.8 \text{ MHz}, & \gamma_{31} &\approx 1000 \text{ Hz}. \end{aligned} \quad (6)$$

In addition, we assume that  $\mathcal{N}_a \approx 1.79 \times 10^{11} \text{ cm}^{-3}$ , then  $\kappa_{12}$  takes the value  $1.0 \times 10^{10} \text{ cm}^{-1} \text{ s}^{-1}$ . The solid and dashed lines in Fig. 1(b) correspond, respectively, to the absence ( $\Omega_c = 0$ ) and the presence ( $\Omega_c = 40 \text{ MHz}$ ) of the control field. We see that in the absence of  $\Omega_c$  the probe field has a large absorption [solid line in Fig. 1(b)] (i.e., no EIT); however, in the presence of  $\Omega_c$  a transparency window is opened in  $\text{Im}(K)$  [dashed line in Fig. 1(b)], and hence the probe pulse can propagate in the resonant atomic system with negligible absorption (i.e., EIT). The openness of the EIT transparency window is due to the quantum interference effect induced by the control field.

At second order, the divergence-free condition requires that

$$\frac{\partial F}{\partial z_1} + \frac{1}{V_g} \frac{\partial F}{\partial t_1} = 0, \quad (7)$$

with  $V_g = (\partial K / \partial \omega)^{-1}$  being the group velocity of  $F$ . The second-order solution reads  $\sigma_{21}^{(2)} = A_{21}^{(2)} (\partial F / \partial t_1) e^{i\theta}$ ,  $\sigma_{31}^{(2)} = A_{31}^{(2)} (\partial F / \partial t_1) e^{i\theta}$ ,  $\sigma_{11}^{(2)} = A_{11}^{(2)} |F|^2 e^{-2\bar{\alpha}z_2}$ ,  $\sigma_{33}^{(2)} = A_{33}^{(2)} |F|^2 e^{-2\bar{\alpha}z_2}$ ,  $\sigma_{32}^{(2)} = A_{32}^{(2)} |F|^2 e^{-2\bar{\alpha}z_2}$ , with

$$A_{21}^{(2)} = \frac{i}{\kappa_{12}} \left( \frac{1}{V_g} - \frac{1}{c} \right), \quad (8a)$$

$$A_{31}^{(2)} = \frac{i}{\Omega_c^*} \left[ -\frac{\omega + d_{31}}{D(\omega)} - \frac{\omega + d_{21}}{\kappa_{12}} \left( \frac{1}{V_g} - \frac{1}{c} \right) \right], \quad (8b)$$

$$A_{11}^{(2)} = \frac{[i\Gamma_{23} - 2|\Omega_c|^2 M]N - i\Gamma_{12} \left( \frac{|\Omega_c|^2}{D(\omega)^* d_{32}^*} - \frac{|\Omega_c|^2}{D(\omega) d_{32}} \right)}{-\Gamma_{12}\Gamma_{23} - i\Gamma_{12}|\Omega_c|^2 M}, \quad (8c)$$

$$A_{33}^{(2)} = \frac{1}{i\Gamma_{12}} (N - i\Gamma_{12} A_{11}^{(2)}) |F|^2 e^{-2\bar{\alpha}z_2}, \quad (8d)$$

$$A_{32}^{(2)} = \frac{1}{d_{32}} \left( -\frac{\Omega_c}{D(\omega)} + 2\Omega_c A_{33}^{(2)} + \Omega_c A_{11}^{(2)} \right), \quad (8e)$$

where  $\bar{\alpha} = \epsilon^{-2}\alpha = \epsilon^{-2}\text{Im}[K(\omega)]$ ,  $M = 1/d_{32} - 1/d_{32}^*$ , and  $N = (\omega + d_{31}^*)/D(\omega)^* - (\omega + d_{31})/D(\omega)$ .

With the above result we proceed to third order. The divergence-free condition in this order yields the nonlinear equation for  $F$ ,

$$i \frac{\partial F}{\partial z_2} - \frac{1}{2} K_2 \frac{\partial^2 F}{\partial t_1^2} - W e^{-2\bar{\alpha}z_2} |F|^2 F = 0, \quad (9)$$

where  $K_2 \equiv \partial^2 K / \partial \omega^2$  and  $W = -\kappa_{12} [\Omega_c^* A_{32}^{(2)} + (\omega + d_{31})(2A_{11}^{(2)} + A_{33}^{(2)})] / D(\omega)$  are dispersion and nonlinear (Kerr) coefficients, respectively.

## B. Ultraslow optical solitons

Combining Eqs. (7) and (9) and returning to the original variables we obtain

$$i \left( \frac{\partial}{\partial z} + \alpha \right) U - \frac{K_2}{2} \frac{\partial^2 U}{\partial \tau^2} - W |U|^2 U = 0, \quad (10)$$

where  $\tau = t - z/V_g$  and  $U = \epsilon F e^{-\bar{\alpha}z_2}$ . Due to the resonant character of the system, the NLS equation, (10), has complex coefficients. Generally, this equation does not allow soliton solution. However, if the imaginary part of the coefficients can be made much smaller than their real part, it is possible to form solitons in the system. We show below that this can indeed be achieved in the present EIT system.

For ultracold Rydberg atoms with the energy levels assigned by (5) and the system parameters given by (6), we obtain  $K_0 = (0.23 + i0.0002) \text{ cm}^{-1}$ ,  $K_1 = (1.15 + i0.0009) \times 10^{-7} \text{ cm}^{-1} \text{ s}$ ,  $K_2 = (1.82 + i0.05) \times 10^{-15} \text{ cm}^{-1} \text{ s}^2$ , and  $W = (2.59 + i0.002) \times 10^{-18} \text{ cm}^{-1} \text{ s}^2$  when selecting  $\Delta_2 = 700 \text{ MHz}$ ,  $\Delta_3 = 2 \text{ MHz}$ ,  $\kappa_{12} = 1 \times 10^{10} \text{ cm}^{-1} \text{ s}^{-1}$ , and  $\Omega_c = 300 \text{ MHz}$ . We see that the imaginary parts of the coefficients of the NLS equation, (10), are indeed much smaller than their corresponding real parts. As a result, Eq. (10) can be approximated as the dimensionless form

$$i \frac{\partial u}{\partial s} + \frac{\partial^2 u}{\partial \sigma^2} + 2u|u|^2 = i\nu u, \quad (11)$$

with  $s = -z/(2L_D)$ ,  $\sigma = \tau/\tau_0$ ,  $u = U/U_0$ , and  $\nu = 2L_D/L_A$ . Here  $L_D \equiv \tau_0^2/|\tilde{K}_2|$ ,  $L_A \equiv 1/(2\alpha)$ , and  $U_0 \equiv (1/\tau_0)\sqrt{|\tilde{K}_2/\tilde{W}|}$  are the characteristic dispersion length, absorption length, and Rabi frequency of the probe field, respectively. Note that in order to obtain soliton solutions we have assumed that  $L_D$  is equal to  $L_{\text{NL}} \equiv 1/(U_0^2 \tilde{W})$  (the characteristic nonlinearity length). The tilde symbol means taking the real part [e.g.,  $\tilde{K}_2 = \text{Re}(K_2)$ ].

When taking  $\tau_0 = 1.0 \times 10^{-7} \text{ s}^{-1}$ , we obtain  $U_0 = 2.65 \times 10^8 \text{ s}^{-1}$ ,  $L_D = L_{\text{NL}} = 5.48 \text{ cm}$ , and  $L_A = 2500 \text{ cm}$ . Because  $L_A$  is much larger than  $L_D$  and  $L_{\text{NL}}$ , which gives  $\nu = 0.0044$ , the absorption term on the right-hand side of Eq. (11) can be neglected in the leading-order approximation. Thus we obtain a standard NLS equation that is completely integrable and allows various soliton solutions. After returning to the original variables, the half-Rabi frequency of the probe field corresponding to single-soliton solution reads

$$\Omega_p(z, t) = \frac{1}{\tau_0} \sqrt{\frac{\tilde{K}_2}{\tilde{W}}} \text{sech} \left[ \frac{1}{\tau_0} \left( t - \frac{z}{\tilde{V}_g} \right) \right] \exp \left[ i\tilde{K}_0 z - i\frac{z}{2L_D} \right], \quad (12)$$

where  $\tilde{K}_0 = \tilde{K}(\omega)|_{\omega=0}$ . With the above system parameters, we obtain

$$\tilde{V}_g = 3 \times 10^{-4} c; \quad (13)$$

i.e., the soliton has an ultraslow propagating velocity, which is essential for its storage and retrieval considered in the next section.

Shown in Fig. 2(a) is the numerical result of the wave shape  $|\Omega_p/U_0|^2$  of the ultraslow optical soliton as a function of  $z/L_D$  and  $t/\tau_0$ . When making the calculation, Eq. (11) is used, with solution (12) as an initial condition. Figure 2(b) shows

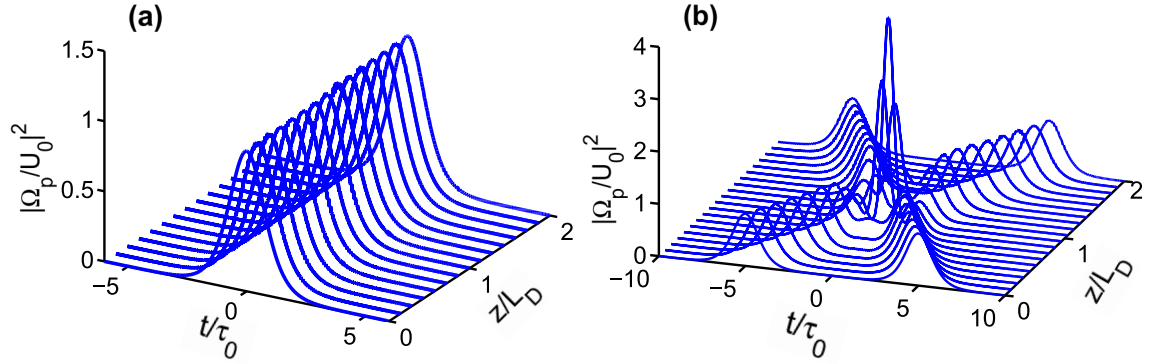


FIG. 2. (Color online) Propagation of an ultraslow optical soliton and the interaction between two solitons. (a) Waveshape  $|\Omega_p/U_0|^2$  of the ultraslow optical soliton as a function of  $z/L_D$  and  $t/\tau_0$ . (b) Collision between two ultraslow optical solitons.

the collision between two ultraslow optical solitons, with the initial condition given by  $u(0, \sigma) = \text{sech}(\sigma - 5) \exp(-i\sigma) + \text{sech}(\sigma + 5) \exp(i\sigma)$ . We see that the ultraslow optical solitons are robust during the propagation and the collision.

It is easy to calculate the threshold of the optical power density  $P_{\max}$  for generating the ultracold optical soliton predicted above by using Poynting's vector [20]. We obtain

$$P_{\max} = 9.38 \times 10^{-5} \text{ W}. \quad (14)$$

Thus, to generate ultraslow optical solitons in the system, a very low input power is needed.

#### IV. STORAGE AND RETRIEVAL OF ULTRASLOW OPTICAL SOLITONS

In a pioneer work [2], Fleischhauer and Lukin showed the possibility of the storage and retrieval of optical pulses in a three-level atomic system with a  $\Lambda$ -type level configuration. They demonstrated that, when switching on the control field, the probe pulse propagates in the atomic medium with nearly vanishing absorption; by slowly switching off the control field the probe pulse disappears and gets stored in the form of atomic coherence; when the control field is switched on again the probe pulse reappears. However, the intensity of the probe pulse used in Ref. [2] and a series of studies carried out later on (see Refs. [3–15] and references therein) is weak; i.e., systems used in those studies [2–15] work in the linear regime. Now we extend these studies into a weakly nonlinear regime and demonstrate that it is possible to realize the storage and retrieval of ultraslow optical solitons in the ladder-type atomic system via EIT.

To this end, we consider the solution of the MB equations presented in Sec. II. We stress that for the storage and retrieval of optical solitons the dynamics of the control field must be taken into account; i.e., Eq. (2b) must be solved together with Eqs. (1) and (2a). Because in this case analytical solutions are not available, we resort to numerical simulation.

Figure 3 shows the time evolution of  $|\Omega_p \tau_0|$  and  $|\Omega_c \tau_0|$  as functions of  $z$  and  $t$  for different input light intensities. In the simulation, the switching-on and the switching-off of the

control field are modeled by the combination of two hyperbolic tangent functions with the form

$$\Omega_c(0, t) = \Omega_{c0} \left\{ 1 - \frac{1}{2} \tanh \left[ \frac{t - T_{\text{off}}}{T_s} \right] + \frac{1}{2} \tanh \left[ \frac{t - T_{\text{on}}}{T_s} \right] \right\}, \quad (15)$$

where  $T_{\text{off}}$  and  $T_{\text{on}}$  are, respectively, the times of switching-off and switching-on of the control field with a switching time approximately given by  $T_s$ . The system parameters are chosen from a typical cold alkali  $^{87}\text{Rb}$  atomic gas with  $\Gamma_{12}/2\pi = 6 \text{ MHz}$ ,  $\Gamma_{23}/2\pi = 3.2 \text{ kHz}$ ,  $\gamma_{21}\tau_0 \approx 1.88$ ,  $\gamma_{31}\tau_0 \approx 10^{-4}$ ,  $\Delta_2\tau_0 = 70$ ,  $\Delta_3\tau_0 = 0.2$ ,  $\kappa_{12}\tau_0 = 1 \times 10^3 \text{ cm}^{-1}$ ,  $\kappa_{23}\tau_0 = 2 \times 10^3 \text{ cm}^{-1}$ ,  $\Omega_{c0}\tau_0 = 30$ ,  $T_s/\tau_0 = 0.2$ ,  $T_{\text{off}}/\tau_0 = 5$ , and  $T_{\text{on}}/\tau_0 = 10$ , with  $\tau_0 = 10^{-7} \text{ s}$ . The wave shape of the input probe pulse is taken as a hyperbolic secant one, i.e.,  $\Omega_p(0, t) = \Omega_{p0} \text{sech}(t/\tau_0)$ , with different  $\Omega_{p0}$  to represent weak (i.e., linear), soliton (i.e., weak nonlinear), and strong probe regimes. Lines 1 to 5 are for  $z = 0, 3, 6, 9$ , and  $12 \text{ cm}$ , respectively.

Shown in Fig. 3(a) is the result for a weak (i.e., linear) probe pulse, where  $\Omega_p(0, t)\tau_0 = 5 \text{sech}(t/\tau_0)$ . In this case, the system is dispersion dominant. Storage and retrieval of light pulses are possible, but the probe pulse broadens rapidly before and after the storage, which is not desirable for practical applications because light information will be lost after storage.

Figure 3(b) shows the result for a weak nonlinear (i.e., soliton) probe pulse, where  $\Omega_p(0, t)\tau_0 = 10 \text{sech}(t/\tau_0)$ . In this situation, the system works in the regime with a balance between dispersion and nonlinearity. We see that, first, the probe pulse evolves into a soliton (i.e., its pulse width is narrowed) before the storage; later the soliton is stored in the atomic medium (i.e.,  $\Omega_p = 0$  when  $\Omega_c$  is switched off); and then the soliton is retrieved after the storage (when  $\Omega_c$  is switched on). The retrieved soliton has nearly the same wave shape as that before storage.

Shown in Fig. 3(c) is the result for a strong probe pulse, where  $\Omega_p(0, t)\tau_0 = 15 \text{sech}(t/\tau_0)$ . In this case, the system works in a strong nonlinear (i.e., nonlinearity-dominant) regime and hence a stable soliton is not possible. From the figure we see that the probe pulse has a significant distortion; especially, some new peaks are generated. Due to the large



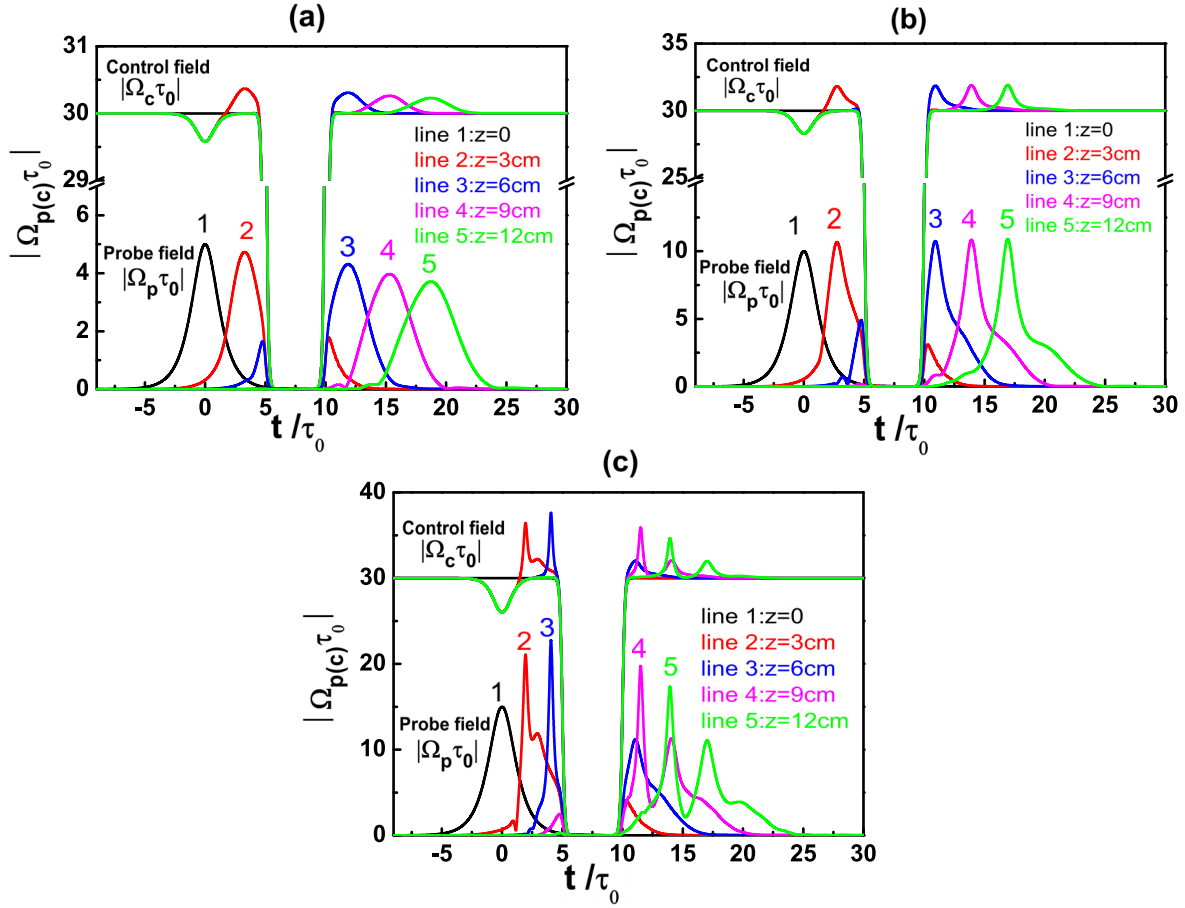


FIG. 3. (Color online) Time evolution of  $|\Omega_p\tau_0|$  and  $|\Omega_c\tau_0|$  as functions of  $z$  and  $t$  for different input light intensities. (a) Storage and retrieval of a weak (i.e., linear) pulse, with  $\Omega_p(0, t)\tau_0 = 5 \text{ sech}(t/\tau_0)$ . (b) Storage and retrieval of a soliton pulse, with  $\Omega_p(0, t)\tau_0 = 10 \text{ sech}(t/\tau_0)$ . (c) Storage and retrieval of a strong pulse, with  $\Omega_p(0, t)\tau_0 = 15 \text{ sech}(t/\tau_0)$ . Lines 1 to 5 in each panel correspond to  $z = 0, 3, 6, 9,$  and  $12$  cm, respectively.

distortion, the light information will be lost rapidly even before storage.

From the result in Fig. 3, we conclude that, compared with the linear pulse and the strong nonlinear pulse, the soliton pulse is desirable for storage and retrieval. One may ask the question how the optical soliton is stored in the atoms when both the probe and the control fields have a vanishing value. In fact, during the light storage the probe-field energy is converted into atomic degrees of freedom; i.e., the atomic coherence  $\sigma_{13}$  has a nonvanishing value even when both  $\Omega_c$  and  $\Omega_p$  are 0.

Shown in Fig. 4 is the result of  $\sigma_{13}$  for different input light intensities as functions of  $z$  and  $t$ . The corresponding evolution of  $|\Omega_c\tau_0|$  is also plotted. Initial probe pulses used in each panel

are the same as those used in Fig. 3. Lines 1 to 5 in each panel correspond to  $z = 0, 3, 6, 9,$  and  $12$  cm, respectively. From Fig. 4 combined with Fig. 3 we see that indeed  $\sigma_{13} \neq 0$  in the time interval when  $\Omega_c = \Omega_p = 0$ . Since the probe pulse is stored in the form of atomic coherence  $\sigma_{13}$  when the control field is switched off and is retained until the control field is switched on again, the atomic coherence  $\sigma_{13}$  can be taken as the intermediary for the storage and retrieval of the probe pulse.

Now we give a simple explanation of the numerical result given above. Note that when the control pulse is switched off, the probe pulse becomes nearly 0. Thus in the weak nonlinear regime, the probe pulse can be approximated as

$$\Omega_p(z, t) \approx \begin{cases} \frac{A}{\tau_0} \sqrt{\frac{\tilde{K}_2}{W}} \text{sech}\left[\frac{1}{\tau_0}\left(t - \frac{z}{v_g}\right)\right] e^{i[\tilde{K}_0 - 1/(2LD)]z} & \text{for } t < T_{\text{off}}, \\ 0 & \text{for } T_{\text{off}} \leq t \leq T_{\text{on}}, \\ \frac{B}{\tau_0} \sqrt{\frac{\tilde{K}_2}{W}} \text{sech}\left[\frac{1}{\tau_0}\left(t - \frac{z}{v_g}\right)\right] e^{i[\tilde{K}_0 - 1/(2LD)]z + i\phi_0} & \text{for } t > T_{\text{on}}, \end{cases} \quad (16)$$

where  $A$  and  $B$  are constants depending on the initial condition and  $\phi_0$  is a constant phase factor.

From both Figs. 3 and 4, we see that the control field is changed before and after storage of the probe field. To

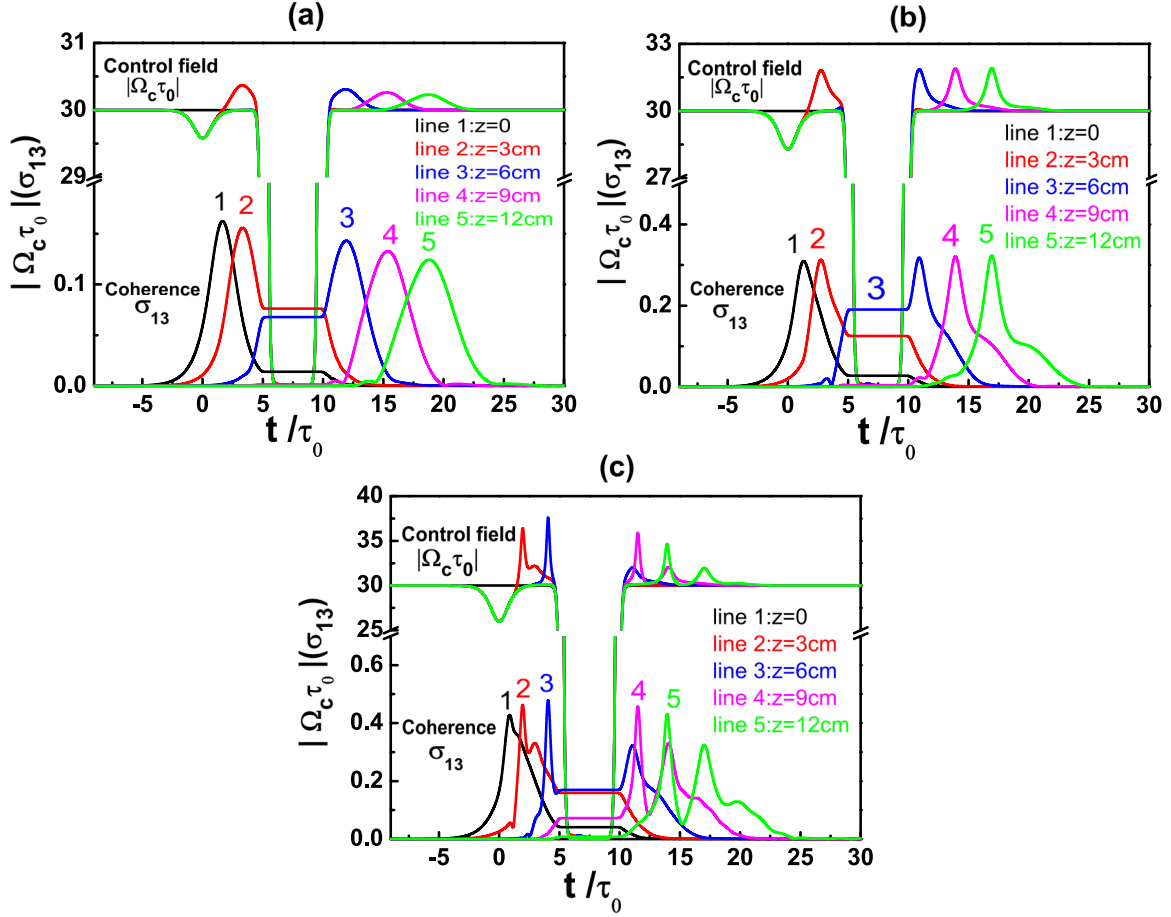


FIG. 4. (Color online) Atomic coherence  $\sigma_{13}$  as a function of distance  $z$  and time  $t$  for different input light intensities. The corresponding evolution of  $|\Omega_c \tau_0|$  is also shown. Initial probe pulses used in (a), (b), and (c) are the same as those used in Figs. 3(a)–3(c), respectively. Lines 1 to 5 in each panel correspond to  $z = 0, 3, 6, 9,$  and  $12$  cm, respectively.

analyze the dynamics (depletion) of the control field before and after storage of the probe soliton, we solve Eq. (2b) using a perturbation method. The numerical result shown in Figs. 3 and 4 suggests making the perturbation expansion

$$\Omega_c = \Omega_c^{(0)} + \epsilon \Omega_c^{(1)} + \epsilon^2 \Omega_c^{(2)}, \quad (17)$$

which is valid for the time interval before and after probe soliton storage where the leading order of  $\Omega_c$  (i.e.,  $\Omega_c^{(0)}$ ) has a large value. Substituting expansion (17) into Eq. (2b) and solving the equations for  $\Omega_c^{(l)}$  ( $l = 0, 1, 2$ ), we obtain the following conclusions. (i)  $\Omega_c^{(0)}$  is a constant, which corresponds to the horizontal line in the upper part of Figs. 3 and 4. (ii)  $\Omega_c^{(1)}(t, z) = \Omega_c^{(1)}(t - z/c)$  describes a hole below the horizontal line in the upper part of Figs. 3 and 4, which propagates at velocity  $c$  (i.e., the light speed in vacuum). The concrete form of  $\Omega_c^{(1)}$  relies on the initial condition. (iii)  $\Omega_c^{(2)}$  satisfies the equation  $i \partial \Omega_c^{(2)} / \partial z = -\kappa_{23} \sigma_{32}^{(2)}$ . Thus we obtain

$$\Omega_c^{(2)} = i \frac{\kappa_{23} \Delta_3}{(|\Omega_c| - \Delta_2 \Delta_3)^2} \frac{1}{\tau_0^2} \frac{\tilde{K}_2}{\tilde{W}} \tanh \left[ \frac{1}{\tau_0} \left( t - \frac{z}{\tilde{V}_g} \right) \right], \quad (18)$$

which has propagating velocity  $\tilde{V}_g$  and contributes a small hump to the horizontal line in the upper part of Figs. 3

and 4. That is, the hump propagates at the same velocity as the probe soliton. Physically, the appearance of the control-field hump (depletion) is due to the energy exchange between the control field and the probe field via the atomic system as an intermediary.

In addition, we can also provide a simple theoretical explanation of the behavior observed in Fig. 4(b), where before and after storage of the probe soliton,  $\sigma_{13}$  behaves like a soliton, but during storage it is constant. First, let us consider the time interval before and after storage of the probe soliton where  $\Omega_c \approx \Omega_c^{(0)}$  [for simplicity we neglect the small hump described by Eq. (18)]. In this region, the perturbation expansion given in Sec. III A is still valid. Thus the result obtained there can be used here. From Eqs. (3a) and (3c), evaluated at the center frequency of the probe pulse (i.e.,  $\omega = 0$ ), we obtain

$$\sigma_{13} = -\frac{\Omega_c^*}{D^*(0)} \Omega_p^* \approx -\frac{\Omega_c^{*(0)}}{D^*(0)} \frac{1}{\tau_0} \sqrt{\frac{\tilde{K}_2}{\tilde{W}}} \operatorname{sech} \left[ \frac{1}{\tau_0} \left( t - \frac{z}{\tilde{V}_g} \right) \right] \times \exp \left[ -i \tilde{K}_0 z + i \frac{z}{2L_D} \right]. \quad (19)$$

We see that, before and after storage of the probe soliton,  $\sigma_{13}$  is also a soliton with propagating velocity  $\tilde{V}_g$ , as expected.

The behavior of  $\sigma_{13}$  in the time interval during probe soliton storage cannot be explained by using the perturbation theory developed in Sec. III A because in this case  $\Omega_c$  is a small quantity. To solve this problem, we start to consider the Bloch equation, (1), directly [27]. Since  $d_{31}\sigma_{31}$  and  $\Omega_p\sigma_{32}$  are small, by Eq. (1e) we have

$$\sigma_{21} \approx -\frac{i}{\Omega_c} \frac{\partial \sigma_{31}}{\partial t}. \quad (20)$$

Furthermore, since  $\sigma_{11} \approx 1$  and  $\sigma_{22} \approx 0$ , Eq. (1d) gives

$$\sigma_{31} \approx -\frac{\Omega_p}{\Omega_c^*} + \frac{1}{i\Omega_c^*} \left( \frac{\partial}{\partial t} - id_{21} \right) \sigma_{21}. \quad (21)$$

Substituting Eq. (20) into Eq. (21) we obtain

$$\begin{aligned} \sigma_{13} &= -\frac{\Omega_p^*}{\Omega_c} - \frac{1}{|\Omega_c|^2} \left( \frac{\partial}{\partial t} + id_{21} \right) \sigma_{13} \\ &\approx -\frac{\Omega_p^*}{\Omega_c}. \end{aligned} \quad (22)$$

Although in the time interval of the storage both the probe and the control fields tend to 0, the ratio  $\Omega_p^*/\Omega_c$  can maintain a finite constant value, as shown in the numerical simulation presented in Fig. 4. The physical reason is that in our study the system starts from the dark state  $|D\rangle = \Omega_c^*|1\rangle - \Omega_p|3\rangle = \Omega_c^*(|1\rangle - (\Omega_p^*/\Omega_c)^*|3\rangle)$  and it approximately remains in this

dark state during time evolution. As a result, the atomic coherence  $\sigma_{13}$  can have a nonzero value even when both  $\Omega_c$  and  $\Omega_p$  are small.

## V. SUMMARY

In the present contribution, we have proposed a method for obtaining stable nonlinear optical pulses and realizing their storage and retrieval in an ultracold ladder-type three-level atomic gas via EIT. Starting from the MB equations, we have derived an NLS equation governing the evolution of the probe-field envelope. We have shown that optical solitons with an ultraslow propagating velocity and extremely low generation power can be created in the system. Furthermore, we have demonstrated that such ultraslowly propagating, ultralow-light-level optical solitons can be stored and retrieved by switching the control field off and on. Because of the balance between dispersion and nonlinearity, the ultraslow optical solitons are robust during propagation, and hence their storage and retrieval are more desirable than those of linear optical pulses. Our study provides the possibility of realizing light information storage and retrieval by using solitonlike nonlinear optical pulses.

## ACKNOWLEDGMENTS

This work was supported by the NSF–China under Grants No. 11174080 and No. 11105052.

- 
- [1] M. Fleischhauer, A. Imamoglu, and J. P. Marangos, *Rev. Mod. Phys.* **77**, 633 (2005).
- [2] M. Fleischhauer and M. D. Lukin, *Phys. Rev. Lett.* **84**, 5094 (2000).
- [3] C. Liu, Z. Dutton, C. Behroozi, and L. Hau, *Nature* **409**, 490 (2001).
- [4] D. F. Phillips, A. Fleischhauer, A. Mair, R. L. Walsworth, and M. D. Lukin, *Phys. Rev. Lett.* **86**, 783 (2001).
- [5] J. J. Longdell, E. Fraval, M. J. Sellars, and N. B. Manson, *Phys. Rev. Lett.* **95**, 063601 (2005).
- [6] U. Schnorrberger, J. D. Thompson, S. Trotzky, R. Pugatch, N. Davidson, S. Kuhr, and I. Bloch, *Phys. Rev. Lett.* **103**, 033003 (2009).
- [7] R. Zhao, Y. O. Dudin, S. D. Jenkins, C. J. Campbell, D. N. Matsukevich, T. A. B. Kennedy, and A. Kuzmich, *Nat. Phys.* **5**, 95 (2009).
- [8] R. Zhang, S. R. Garner, and L. V. Hau, *Phys. Rev. Lett.* **103**, 233602 (2009).
- [9] A. G. Radnaev, Y. O. Dudin, R. Zhao, H. H. Jen, S. D. Jenkins, A. Kuzmich, and T. A. B. Kennedy, *Nat. Phys.* **6**, 894 (2010).
- [10] Y. O. Dudin, R. Zhao, T. A. B. Kennedy, and A. Kuzmich, *Phys. Rev. A* **81**, 041805(R) (2010).
- [11] F. Yang, T. Mandel, C. Lutz, Z.-S. Yuan, and J.-W. Pan, *Phys. Rev. A* **83**, 063420 (2011).
- [12] I. Novikova, R. L. Walsworth, and Y. Xiao, *Laser Photon. Rev.* **6**, 333 (2012).
- [13] H.-N. Dai, H. Zhang, S.-J. Yang, T.-M. Zhao, J. Rui, Y.-J. Deng, L. Li, N.-L. Liu, S. Chen, X.-H. Bao, X.-M. Jin, B. Zhao, and J.-W. Pan, *Phys. Rev. Lett.* **108**, 210501 (2012).
- [14] Y. O. Dudin, L. Li, and A. Kuzmich, *Phys. Rev. A* **87**, 031801 (2013).
- [15] G. Heinze, C. Hubrich, and T. Halfmann, *Phys. Rev. Lett.* **111**, 033601 (2013).
- [16] T. N. Dey and G. S. Agarwal, *Phys. Rev. A* **67**, 033813 (2003).
- [17] M. Saffman, T. G. Walker, and K. Mølmer, *Rev. Mod. Phys.* **82**, 2313 (2010).
- [18] J. D. Pritchard, K. J. Weatherill, and C. S. Adams, *Annu. Rev. Cold At. Mol.* **1**, 301 (2013).
- [19] Y. Wu and L. Deng, *Opt. Lett.* **29**, 2064 (2004).
- [20] G. Huang, L. Deng, and M. G. Payne, *Phys. Rev. E* **72**, 016617 (2005).
- [21] D. Maxwell, D. J. Szwer, D. Paredes-Barato, H. Busche, J. D. Pritchard, A. Gauguier, K. J. Weatherill, M. P. A. Jones, and C. S. Adams, *Phys. Rev. Lett.* **110**, 103001 (2013).
- [22] J. Gea-Banacloche, Y.-Q. Li, S.-Z. Jin, and M. Xiao, *Phys. Rev. A* **51**, 576 (1995).
- [23] R. W. Boyd, *Nonlinear Optics*, 3rd. ed. (Academic Press, Elsevier, New York, 2008).
- [24] H.-J. Li and G. Huang, *Phys. Lett. A* **372**, 4127 (2008).
- [25] The frequency and wave number of the probe field are given by  $\omega_p + \omega$  and  $k_p + K(\omega)$ , respectively. Thus  $\omega = 0$  corresponds to the center frequency of the probe field.
- [26] J. D. Pritchard, D. Maxwell, A. Gauguier, K. J. Weatherill, M. P. A. Jones, and C. S. Adams, *Phys. Rev. Lett.* **105**, 193603 (2010).
- [27] P. W. Milonni, *Fast Light, Slow Light and Left-Handed Light* (Institute of Physics, Bristol, UK, 2005), sec. 6.2.